International Conference on Control, Engineering & Information Technology (CEIT'13)
Proceedings Engineering & Technology - Vol.3, pp. 57-68,2013
Copyright - IPCO

Fuzzy Load Shedding Strategy Based on the Anticipation of the Point of Voltage Collapse

Kamel Jemaï, Meriame Abderrahim, Hafedh Trabelsi

Abstract— As a perspective to ensure the power system stability and to avoid the vulnerability leading to the blackouts, several strategies are adopted. In order to avoid the voltage collapse, load shedding schemes represent a suitable action to maintain the power system service quality and to control its vulnerability. In this paper, we propose a new approach of a load shedding strategy based on fuzzy controllers. This strategy was founded on the calculation of generated power sensitivity degree related to voltage level at different network buses. During the fault phase, fuzzy controller algorithms generate monitor vectors ensuring a pre-calculated load shedding ratio in the purpose to reestablish the power balance and avoid the appearance of the collapse phenomenon.

***Index Terms*—Load shedding, Fuzzy logic, Synchronous machine, Load flow, Hydraulique turbine.**

I. INTRODUCTION

Various perturbations occur every year in electrical networks that lead to blackouts. One of the major challenges facing network operators of electrical energy is notably the establishment of an optimal quality of service of these networks by ensuring a better quality of powers to different nodes of transit of this network. These objectives can never be achieved if the implementation of efficient control strategies based on an accurate and adequate margin of variation of state variables of the system following the emergence of disturbances fugitive.

As the frequency and voltage represent two important parameters to the power system safety, it should have a continuous control of these parameters and this to ensure the best service quality. It's characterized by standard criterions related to the service continuity, the voltage and the frequency qualities. The network control is an important rivalry, since control strategies can be considered in order to guarantee network service quality. In the case of cascade of events leading to susceptible failures, load shedding action will be most strategic to prevent network instability [1]. Different methods [2], [10] were proposed in order to decide the place and the quantity of loads to be shed. We develop, in this paper, a new fuzzy load shedding strategy.

II. STUDIED MODEL

The studied model is based on the IEEE test 14 buses network, Fig. 1.

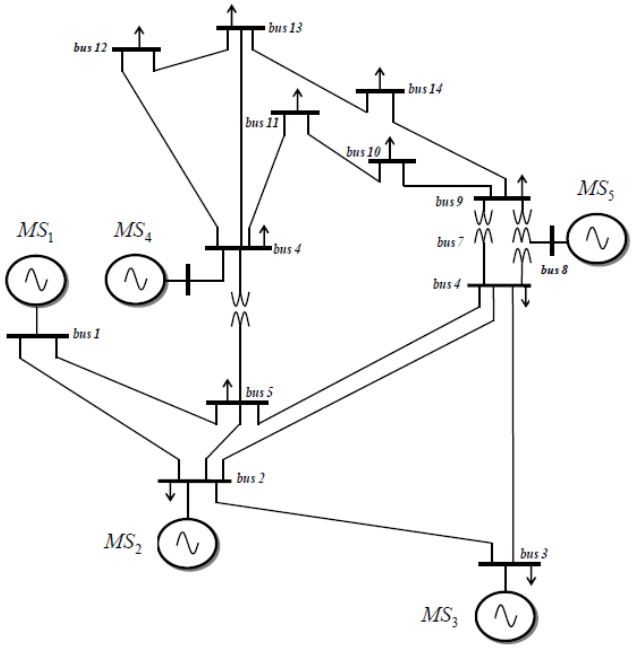

Fig. 1. Studied model: IEEE 14- Bus Network

The dynamic behavior analysis of power system is based on a relevant modeling taking into account the electrodynamics possible states affecting the network in case of serious event appearances [9].

We adopted for the synchronous machines M_{Sk} ; $k = \{1,...,5\}$ a state model of fourth order as:

$$\begin{cases} \dot{E}'_{qk} = \dfrac{1}{T'_{dok}}.[E_{fdk} - E'_{qk} + (X_{dk} - X'_{dk}).i_{dk}] \\ \dot{E}'_{dk} = \dfrac{1}{T'_{qok}}.[-E'_{dk} + (X_{qk} - X'_{qk}).i_{qk}] \\ \dot{\omega}_k = \dfrac{1}{M_k}.[P_{M_k} - P_{SM_k} - D_k.(\omega_k - \omega_{ks})] \\ \dot{\delta}_k = \omega_k - 1 \end{cases} \quad (1)$$

E'_{dk}, E'_{qk} and E_{fdk} are respectively the (d, q) axe transient emf and the emf excitation.

X_{dk}, X_{qk}, X'_{dk} and X'_{qk} are respectively the (d, q) axe reactance and the (d, q) axe transient reactance.

D_k Damping coefficient. M_k Inertia constant.

P_{SM_k}, P_{M_k}, ω_{ks} and δ_k are respectively the electrical power, mechanical power, synchronism speed and the rotor angle.

Each synchronous machine is provided with a speed and voltage regulators [9]. The speed regulator ensures the frequency control of the generator by an adjustment of the mechanical power delivered to the generator according to the network demand. The voltage regulator is based on the detection of the gap between the voltage instantaneous value at machine terminal and a reference value: consequently, we react on the excitation voltage level. The turbine control is assigned to its inlet gate position G_{HT} and that from the equation of dynamics, equations (8), [20]. We implemented a fuzzy controller in order to enslave the process of the gate opening, Fig.2 [5], [7], [13].

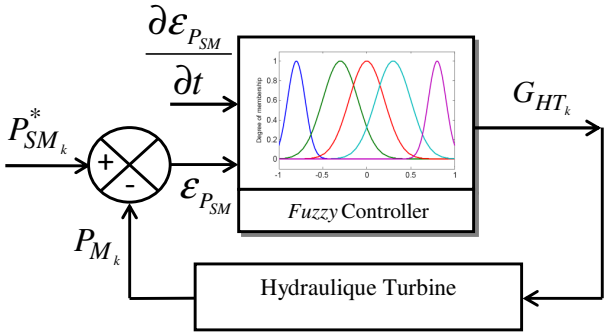

Fig. 2. Control of the gate opening

The reference of the turbine P^*_{SM} is at all times the amount of power consumed P_C and that injected P_{IN} at the point of connection to the network, Fig. 1. In other words:

$$P^*_{SM_k} = P^*_{IN_k} + P_{C_k} \quad (2)$$

To ensure a better quality of powers exchanged between machines and the network we have adopted a new technique to control the frequency fluctuations through the adjustment of mechanical power developed by the hydraulique turbine. Indeed, during the phase of a fault, the active P_{SM_k}, reactive Q_{SM_k} and mechanical P_{M_k} powers exchanged, are strongly fluctuating. The dynamics of synchronous machines will be governed by the following mathematical model:

$$\dot{\omega}_k = \frac{\Delta P_{(SM/M)_k} - D_k.(\omega_k - \omega_{ks})}{M_k} \quad (3)$$

Where:

$$\begin{cases} \Delta P_{(SM/M)_k} = \Delta P_{(SM/M)_k - 0} + \Delta P_{(SM/M)_k - 2.f} \\ \Delta P_{(SM/M)_k - 0} = P_{SM_k - 0} - P_{M_k - 0} \\ \Delta P_{(SM/M)_k - 2.f} = P_{SM_k - 2.f} - P_{M_k - 2.f} \end{cases}$$

$P_{SM_k - 2.f}$, $P_{M_k - 2.f}$ represent respectively the active and mechanical powers fluctuates twice that of the network $2.f$, during the phase fault t_f. Thus, the synchronous machine frequency will range on an interval $[f_k^{\min}, f_k^{\max}]$ described by (4).

$$f_k = \left[\frac{\Delta P_{(SM/M)_k}}{2.\pi.D_k} + f\right].\left[1 - e^{-\frac{t - t_f}{\tau_k}}\right] \quad (4)$$

Where:

$$\tau_k = \frac{M_k}{D_k}$$

Consequently, the implementation of a technical limitation of the mechanical power P_M developed by the turbine is required, Fig. 3.

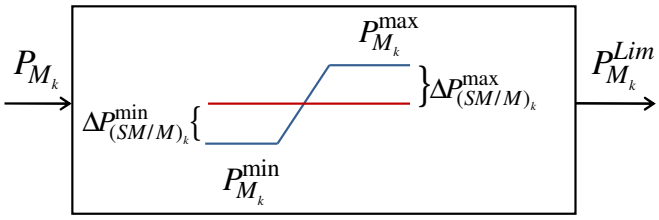

Fig. 3. Power limitation

Where:

$$\begin{cases} \Delta P^{\max}_{(SM/M)_k} = 2.\pi.D_k.\left[\dfrac{f_k^{\max}}{1-e^{-\frac{t-t_f}{\tau_k}}} - f\right] \\ \Delta P^{\min}_{(SM/M)_k} = 2.\pi.D_k.\left[\dfrac{f_k^{\min}}{1-e^{-\frac{t-t_f}{\tau_k}}} - f\right] \end{cases} \quad (5)$$

III. FUZZY LOAD SHEDDING STRATEGY

Disturbances leading to the voltage collapse phenomenon have stochastic characters. In a given bus, if the production source doesn't succeed in compensating the VAR reactive power, voltage level drops. The active and reactive powers injected at bus i (P_{IN_i}, Q_{IN_i}) are expressed as follows:

$$\begin{cases} P_{IN_i} = \sum_{j=1}^{j=N_{bus}} Y_{ij}.V_i.V_j.\cos(\alpha_i - \alpha_j - \theta_{ij}) \\ Q_{IN_i} = \sum_{j=1}^{j=N_{bus}} Y_{ij}.V_i.V_j.\sin(\alpha_i - \alpha_j - \theta_{ij}) \end{cases} \quad (6)$$

Y_{ii} , θ_{ii} : Module and argument of the line admittance ii .

V_i , α_i : Module and argument of voltage at bus i .

V_j , α_j : Module and argument of voltage at bus j .

N_{bus} : Number of studied network buses.

The machine connected at bus i must provide active and reactive powers respectively P_{SM_i} , Q_{SM_i} where:

$$\begin{cases} P_{SM_i} = P_{C_i} + P_{IN_i} \\ Q_{SM_i} = Q_{C_i} + Q_{IN_i} \end{cases} \quad (7)$$

P_{C_i} and Q_{C_i} are respectively active and reactive powers consumed at bus i .

In order to evaluate the influence of the consumed powers level (P_{C_i}, Q_{C_i}) at different buses on the generated power level, we can transform the relations (5), as follows:

$$\begin{cases} \left[P_{IN_i} - Y_{ii}.V_i^2.\cos(\theta_{ii})\right]^2 = \left[\sum_{j=1}^{j=N_{bus}} Y_{ij}.V_i.V_j.\cos(\alpha_i - \alpha_j - \theta_{ij})\right]^2 \\ \left[Q_{IN_i} + Y_{ii}.V_i^2.\sin(\theta_{ii})\right]^2 = \left[\sum_{j=1}^{j=N_{bus}} Y_{ij}.V_i.V_j.\sin(\alpha_i - \alpha_j - \theta_{ij})\right]^2 \end{cases} \quad (8)$$

This leads to:

$$\begin{aligned} & P_{IN_i}^2 - Q_{IN_i}^2 - A_{V2i}.V_i^2 + A_{V4i}.V_i^4 \\ & = A_{\cos i}.V_i^2 - A_{\sin i}.V_i^2 \end{aligned} \quad (9)$$

Where:

$$\begin{cases} A_{V2i} = 2.Y_{ii}.[P_{IN_i}.\cos(\theta_{ii}) + Q_{IN_i}.\sin(\theta_{ii})] \\ A_{V4i} = Y_{ii}^2.[\cos^2(\theta_{ii}) - \sin^2(\theta_{ii})] \\ A_{\cos i} = \sum_{k=1}^{k=N_{bus}} [Y_{ik}.V_k.\cos(\alpha_i - \alpha_k - \theta_{ik})]^2 \\ A_{\sin i} = \sum_{k=1}^{k=N_{bus}} [Y_{ik}.V_k.\sin(\alpha_i - \alpha_k - \theta_{ik})]^2 \end{cases} \quad (10)$$

We set:

$$X_{V2i} = V_i^2$$

Then we obtain:

$$\begin{aligned} A_{V4i}.X_{v2i}^2 + (A_{\sin i} - A_{V2i} - A_{\cos i}).X_{v2i} \\ + P_{IN_i}^2 - Q_{IN_i}^2 = 0 \end{aligned} \quad (11)$$

The critical voltage V_{ic} in a given node i is given by:

$$V_{ic} = \left[-\frac{A_{\sin} - A_{V2} - A_{\cos}}{2.A_{V4}}\right]^{\frac{1}{2}} \quad (12)$$

This development leads us to represent the evolution curve of the power P_{IN_i} injected at a bus i according to the voltage V_i in the same bus. Particular attention will be paid to the critical point (P_{IN_ic}, V_{ic}), i.e. where a voltage collapse is likely to occur, Fig. 4.

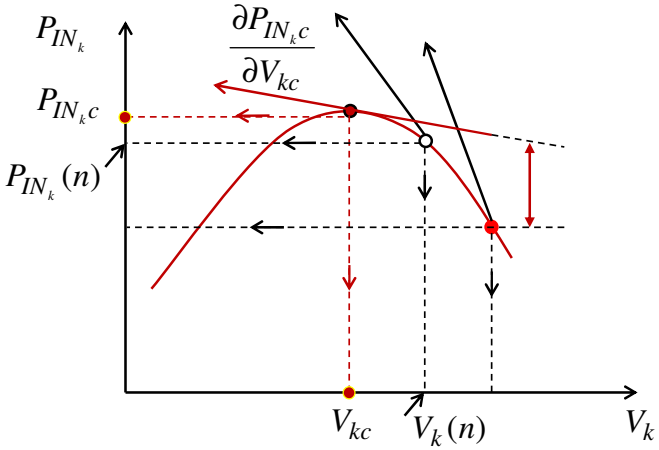

Fig. 4. Estimation of the collapse voltage phenomenon

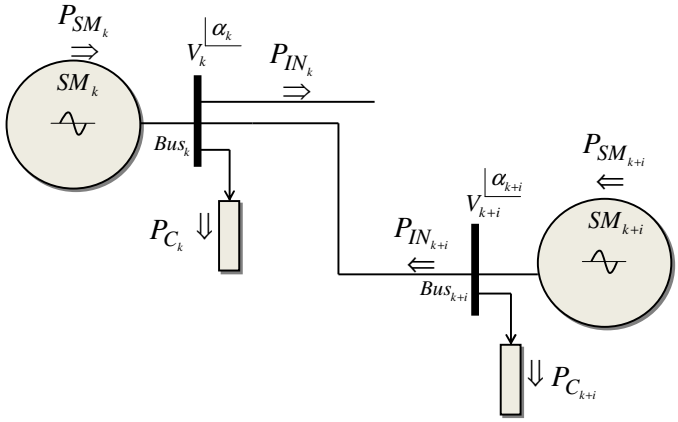

Fig. 5. Powers transit

$P_{IN_k}(n)$, $V_k(n)$ represents the values of the injected power and the voltage at a bus i at the end of a computation step.

In fact, in a given operating point we can estimate the critical slope $\left.\frac{\partial P_{IN_i c}}{\partial V_{ic}}\right|_{(n)}$ by means of the following numerical relation:

$$\left.\frac{\partial P_{IN_i c}}{\partial V_{ic}}\right|_{(n)} = \frac{P_{IN_i c} - P_{IN_i}(n)}{V_i(n) - V_{ic}} \tag{13}$$

Which leads to:

$$\begin{cases} \left.\frac{\partial P_{SM_k}}{\partial V_i}\right|_{(n)} = \left[\frac{\partial P_{C_k}}{\partial V_i} + \frac{\partial P_{IN_k}}{\partial V_i}\right]_{(n)} \\ \left.\frac{\partial Q_{SM_k}}{\partial V_i}\right|_{(n)} = \left[\frac{\partial Q_{C_k}}{\partial V_i} + \frac{\partial Q_{IN_k}}{\partial V_i}\right]_{(n)} \end{cases} \tag{14}$$

Practically, the term $\frac{\partial P_{SM_k}}{\partial V_i}$ represents the impact of voltage fluctuations in a given bus V_i on the power level P_{SM_k} generated by the machine SM_k, Fig. 5.

Also, the term $\left.\frac{\partial P_{SM_k}}{\partial V_i}\right|_{(n)}$ is numerically evaluated as indicated by (15).

$$\begin{cases} \left.\frac{\partial P_{SM_k}}{\partial V_i}\right|_{(n)} = \frac{[P_{C_k} + P_{IN_k}]_{(n)} - [P_{C_k} + P_{IN_k}]_{(n-1)}}{V_i(n) - V_i(n-1)} \\ \left.\frac{\partial Q_{SM_k}}{\partial V_i}\right|_{(n)} = \frac{[Q_{C_k} + Q_{IN_k}]_{(n)} - [Q_{C_k} + Q_{IN_k}]_{(n-1)}}{V_i(n) - V_i(n-1)} \end{cases} \tag{15}$$

Thus, the sensitivity ξ_{SM_k} of a synchronous machine SM_k to random variations of different voltages will be evaluated through the relation (16).

$$\xi_{SM_k} = \sum_{i=1}^{i=N_{bus}} \frac{\partial P_{SM_k}}{\partial V_i} \tag{16}$$

Secondly, we assess this sensitivity before occurrence of faults counted as variable of reference $\xi^*_{SM_k}$:

$$\xi^*_{SM_k} = \sum_{i=1}^{i=N_{bus}} \left.\frac{\partial P_{SM_k}}{\partial V_i}\right|^* \tag{17}$$

Taking into account the difference between the two quantities ξ_{SM_k} and $\xi^*_{SM_k}$, we evaluate the error and its instantaneous variation which will be processed by a fuzzy controller, Fig. 6.

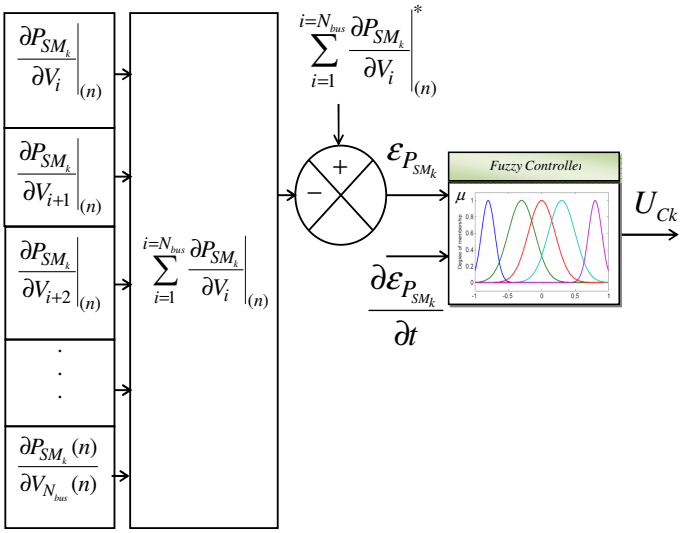

Fig. 6. Fuzzy processing of the sensitivity

The vector U_{Ck} generated by the fuzzy controller must adjust the level of the power consumed in all buses in the studied network, Fig. 7. Specifically, this vector is a global action that needs to be dispatched to all loads:

$$U_{Ck} = \sum_{i=1}^{i=N_{bus}} U_{Ck \to i} \tag{18}$$

Hence:

$$U_{Ck \to i} = \frac{\dfrac{\partial P_{SM_k}}{\partial V_i}}{\sum_{i=1}^{i=N_{bus}} \dfrac{\partial P_{SM_k}}{\partial V_i}} . U_{Ck} \tag{19}$$

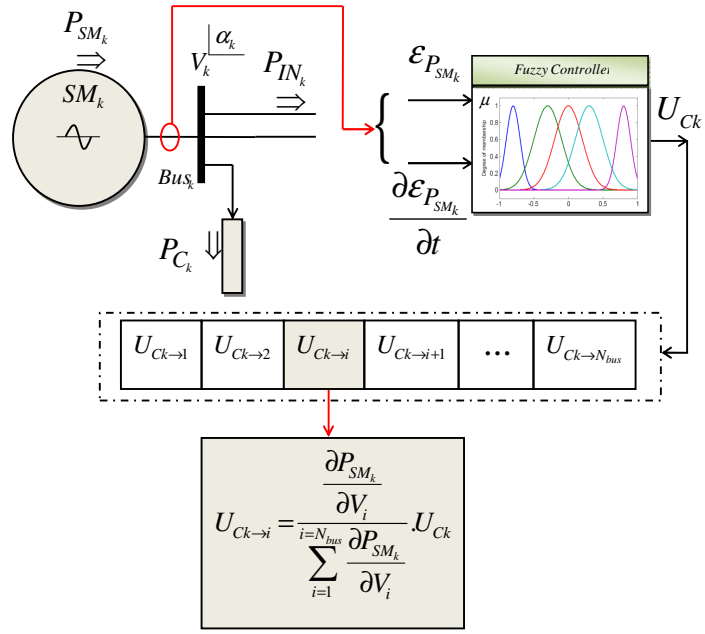

Fig. 7. Fuzzy load shedding

Taking into account the sensitivity of a machine MS_k to a voltage level V_i at a bus i, the value of the power available for consumption in that node would be:

$$P_{Ci}(n) = (1 - U_{Ck \to i}).P_{Ci}(n-1) \tag{20}$$

Thus and taking into account the sensitivity of all the machines to the voltage levels V_i everywhere in the network, the vector generated by a fuzzy controller aiming at an optimized load shedding procedure at a bus i would be evaluated in accordance with the schematic diagram shown in Fig. 8.

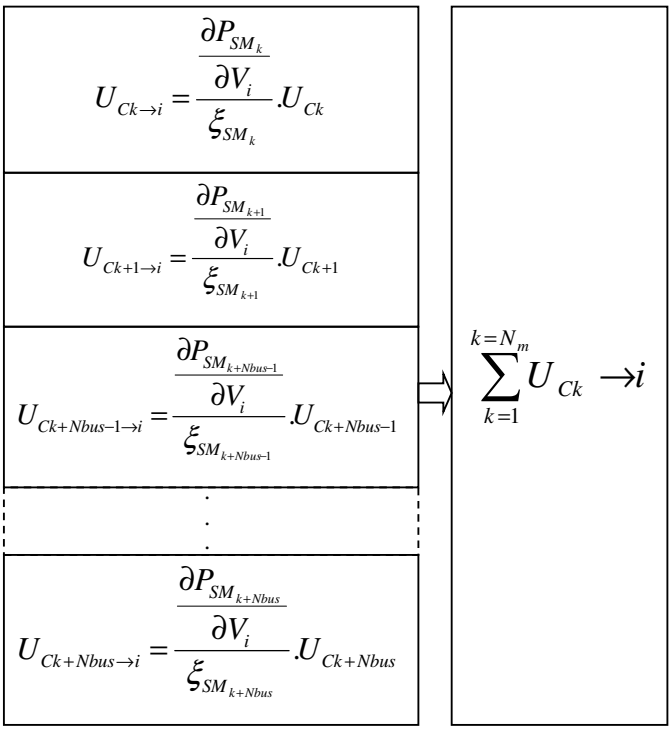

Fig. 8. Fuzzy load shedding procedure at a given node i

For all the loads, the load shedding procedure is summarized in Fig. 9.

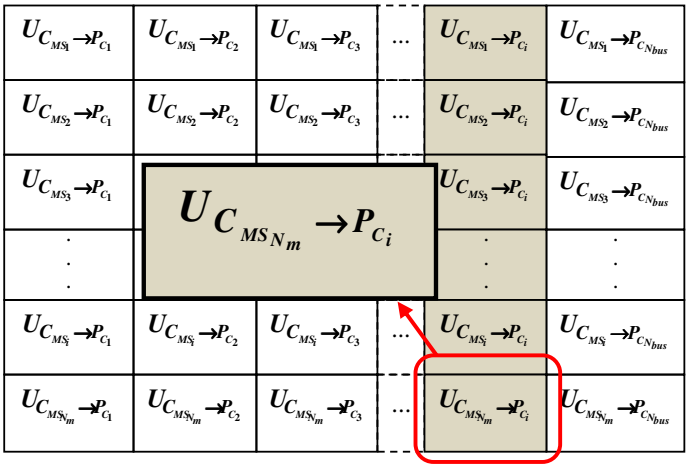

Fig. 9. Overview of the procedure of Fuzzy load shedding

Accordingly, the power level at a bus i depending on the sensitivity of all machines MS_k $k = \{1,...,N_m\}$ is:

$$P_{C_i}(n) = (1 - \sum_{k=1}^{k=N_m} U_{Ck\to i}).P_{C_i}(n-1) \quad (21)$$

A new balance of power is established following this action of load shedding:

$$\sum_{k=1}^{N_m} P_{SM_k} = \sum_{i=1}^{N_{load}} (1 - \sum_{k=1}^{k=N_m} U_{Ck\to i}).P_{C_i} + \sum_{i=1}^{i=N_{bus}} P_{IN_i} \quad (22)$$

At this stage of load shedding procedure, we adjust the specific active power P_{sp_k} at each bus k :

$$\begin{cases} P_{sp_k} = P_{SM_k} - (1 - \sum_{j=1}^{j=N_m} U_{Cj\to k}).P_{C_k} \\ Q_{sp_k} = Q_{SM_k} - Q_{C_k} \end{cases} \quad (23)$$

Then we evaluate the active and reactive power functions $F_{Pk}(V_k, \alpha_k)$ and $F_{Qk}(V_k, \alpha_k)$ as follow:

$$\begin{cases} F_{Pk}(V_k, \alpha_k) = P_{IN_k} - P_{sp_k} \\ F_{Qk}(V_k, \alpha_k) = Q_{IN_k} - Q_{sp_k} \end{cases} \quad (24)$$

The Jacobian matrix $[J]$ is reconstructed by the partial derivatives with respect to modules and arguments of the voltages at different buses ($\frac{\partial F_{Pk}}{\partial \alpha_k}, \frac{\partial F_{Pk}}{\partial V_k}, \frac{\partial F_{Qk}}{\partial \alpha_k}, \frac{\partial F_{Qk}}{\partial V_k}$). It is reconstituted based elementary matrices $[J_{P\alpha}], [J_{PV}]$, $[J_{Q\alpha}]$ and $[J_{QV}]$, and defined as indicated in (25).

$$[J] = \begin{bmatrix} [J_{P\alpha}] & [J_{PV}] \\ [J_{Q\alpha}] & [J_{QV}] \end{bmatrix} \quad (25)$$

We increment the vector of desired variables $[X]=[V_k,\alpha_k]$ at each step of calculation in accordance with the following relation:

$$[X]_{(n+1)}=[X]_{(n)}-[J]^{-1}.\begin{bmatrix} FP_2 \\ FP_3 \\ . \\ \dot{FP}_N \\ FQ_2 \\ FQ_3 \\ . \\ FQ_N \end{bmatrix} \quad (26)$$

We have established, under the MATLAB environment, a program for calculating the network load flow in accordance with the following algorithm.

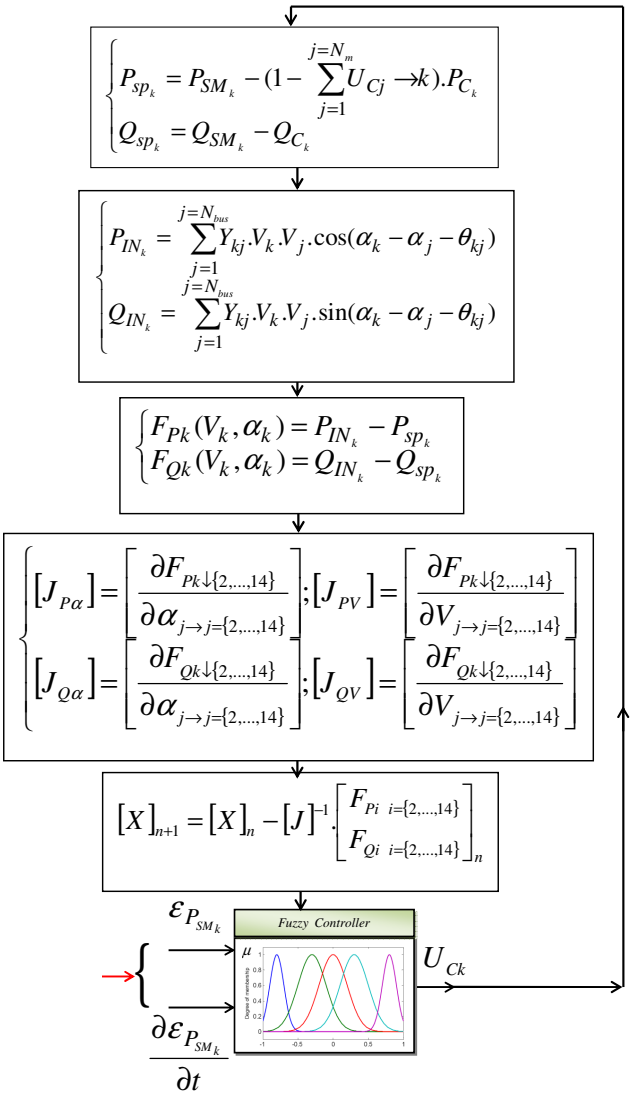

Fig. 10. Algorithm of calculation

IV. Studied Model of a Fuzzy Controller

The topology of each fuzzy controller to integrate in the fuzzy bi-clustering technique was based on an interaction between two input variables, successively characterized by an error ε_i and an instantaneous variation $\partial\varepsilon_i/\partial t$ of this error, to synthesize a control vector U_{Cfi} acting on one of the state variables of the power system studied [5], [7], and [12]. Indeed, we have implemented the matrix of fuzzy inference by means of a number of membership functions MF_i, both for the error ε_i, for variation of the error $\partial\varepsilon_i/\partial t$ and for the control vector U_{Cfi}, equal to nine, (26). Thus, the total number of fuzzy inferences N_{rulers} amounts to 81, table IV, thus giving a better accuracy with the decision taken by the regulator specified [20], [22].

$$MF_i=\left\{\begin{matrix} MF_{NVL}, MF_{NL}, MF_{NM}, \\ MF_{NS}, MF_{ZE}, MF_{PS}, \\ MF_{PM}, MF_{PL}, MF_{PVL} \end{matrix}\right\} \quad (27)$$

Where:
NVL : Negative Very Large, NL : Negative Large,
NM : Negative Medium, NS : Negative Small,
ZE : Zero, PS : Positive Small, PM : Positive Medium,
PL : Positive Large, PVL : Positive Very Large.

Based on the degree of membership $\mu_{\varepsilon_i-MF_i}$ of the error ε_i and the degree of membership $\mu_{\frac{\partial\varepsilon_i}{\partial t}-MF_i}$ of the variation of the error we deduce the control vector U_{Cfi}, Fig. 11.

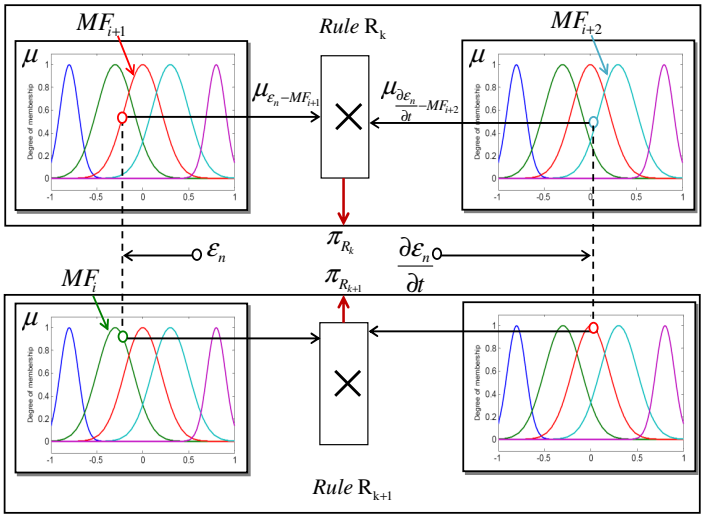

Fig. 11. Fuzzy deductions

The quantities are treated as follow:

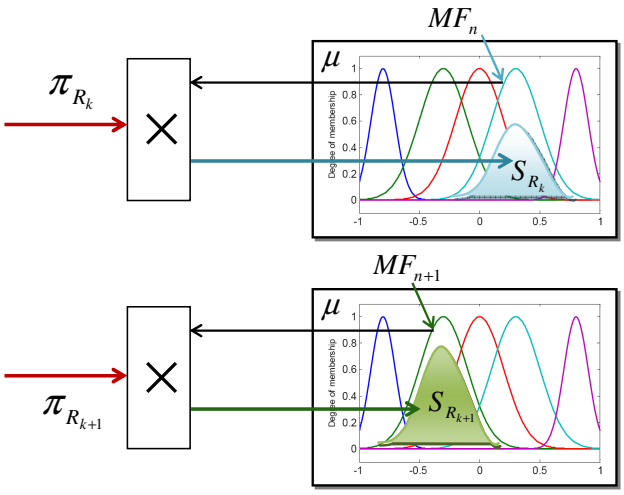

Fig. 12. Fuzzy surfaces

The indicated surface, S_{Rk} and S_{Rk+1} related to the rules R_k and R_{k+1} are given by the following relations:

$$\begin{cases} S_{Rk} = \Pi_{R_k}.MF_n \\ S_{Rk+1} = \Pi_{R_{k+1}}.MF_{n+1} \end{cases} \quad (28)$$

The global surface sweep by the fuzzy control vector is indicated by Fig. 13.

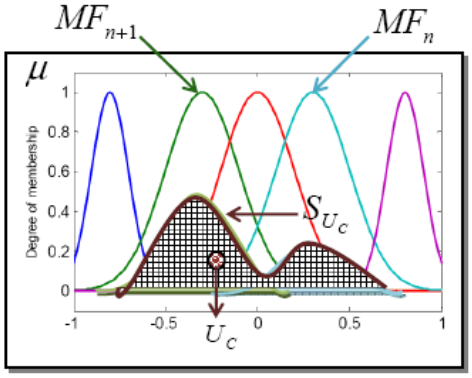

Fig. 13. Control vector deduction

Where:

$$S_{U_C} = \frac{S_{Rk} + S_{Rk+1}}{N_{Rk}} \quad (29)$$

Based on the fact that we have considered nine membership functions, $\{MF_1,...,MF_n\}; n = 9$, both the error and the variation of the error, the area SU_{Cfi} swept by the control vector generated by the specified controller, according to fuzzy rules adopted, is evaluated as follows:

$$\begin{cases} SU_{Cfi} = \sum_{k=1}^{k=N_{rulers}} \frac{\Pi_{Rk}.MF_i(U_{Cfi})\big|_{R_k}}{N_{rulers}} \\ \Pi_{Rk} = \mu_{\varepsilon_i - MF_i}\big|_{R_k}.\mu_{\frac{\partial\varepsilon_i}{\partial t} - MF_i}\Big|_{R_k} \end{cases} \quad (30)$$

Therefore, the fuzzy vector U_{Cfi} generated, Fig. 12, is none other than the abscissa of the centre of gravity of this surface SU_{Cfi}. Then:

$$U_{Cfi} = \frac{\int_{-1}^{1} \Pi_{Rk}.MF_i(U_{Cfi})}{\int_{-1}^{1} \Pi_{Rk}} \quad (31)$$

A technique of scaling will be of great importance for the amplitudes of the control variables that may possibly exceed the extreme limits quoted. In other words, all sizes to be treated X_i giving rise to an error $\varepsilon_i(t)$ and a variation of error $\frac{\partial\varepsilon_i(t)}{\partial t}$, must undergo a transfer at the base of fuzzy variables evidenced by the interval $[-1, 1]$, to generate the fuzzy input $[\varepsilon_{fi}(t)$ and $\frac{\partial\varepsilon_{fi}(t)}{\partial t}]$ required for processing by the designated controller in accordance with the following system of equations:

$$\begin{cases} \varepsilon_{fi} = K_{\varepsilon_i}.\varepsilon_i(t) + [1 - K_{\varepsilon_i}] \\ \frac{\partial\varepsilon_{fi}}{\partial t} = K_{\frac{\partial\varepsilon_i}{\partial t}}.\frac{\partial\varepsilon_i(t)}{\partial t} + [1 - K_{\frac{\partial\varepsilon_i}{\partial t}}] \\ K_{\varepsilon_i} = \frac{2}{B_{max}(E_{F-\varepsilon fi}) - B_{min}(E_{F-\varepsilon fi})} \\ K_{\frac{\partial\varepsilon_i}{\partial t}} = \frac{2}{B_{max}(E_{F-\frac{\partial\varepsilon fi}{\partial t}}) - B_{min}(E_{F-\frac{\partial\varepsilon fi}{\partial t}})} \end{cases} \quad (32)$$

Similarly, the control vector U_{Cfi} must undergo a transfer to the basic quantities studied (per unit) to assign the value U_{Ci} and this means the system of equations:

$$\begin{cases} U_{Ci} = K_{U_{Ci}}.U_{Cfi} + [1 - K_{U_{Ci}}] \\ K_{U_{Ci}} = \dfrac{B_{max}(E_{F-U_{Cfi}}) - B_{min}(E_{F-U_{Cfi}})}{2} \end{cases} \quad (33)$$

Through this new technique of rescaling, we assigned a dynamic behavior to the fuzzy controller in order to ensure better tracking of the variable to control.

V. Criterion of the Stability Analysis

The study of the stability of a synchronous machine MS_k adopted was based on the evaluation of the eigen values of the state model selected from a state vector $[X_k]$ characterized by dynamic variables $[\delta_k, \omega_k, E'_{qk}, E'_{dk}]$ (1) and a control vector $[Y_k]$ characterized by the algebraic variables $[V_k, \alpha_k]$ all related to the specified machine.

By referring to the dynamics of a synchronous machine MS_k as well as the assessment of the powers at the node where it is connected, we write:

$$\begin{cases} [\dot{X}_{ik}] = F_k(X_k, Y_k) \\ [0] \quad = G_k(X_k, Y_k) \end{cases} \quad (34)$$

It then comes:

$$\begin{cases} \Delta[\dot{X}_k] = [A_k^1].\Delta[X_k] + [B_k^1].\Delta[Y_k] \\ [0] \quad = [A_k^2].\Delta[X_k] + [B_k^2].\Delta[Y_k] \end{cases} \quad (35)$$

The matrix $[A_k^1], [B_k^1]$, $[A_k^2]$ and $[B_k^2]$ had dimensions respectively $[4\times4]$, $[4\times2]$, $[2\times4]$ and $[2\times2]$, their coefficients can be deduced without particular difficulty from the following partial derivatives:

$$\begin{cases} [A_k^1] = \left[\dfrac{\partial F_k}{\partial X_k}\right] \quad ; \quad [B_k^1] = \left[\dfrac{\partial F_k}{\partial X_k}\right] \\ [A_k^2] = \left[\dfrac{\partial G_k}{\partial X_k}\right] \quad ; \quad [B_k^2] = \left[\dfrac{\partial G_k}{\partial X_k}\right] \end{cases} \quad (36)$$

A transformation of (35) leads to:

$$\Delta[\dot{X}_k] = [A_k].\Delta[X_k] \quad (37)$$

According to the signs of the real parts of n , $\mathrm{n} = \{1,...,4\}$ eigen values λ_k^n of the matrix $[A_k]$, of dimensions $[4\times4]$, we decide on the stability of the machine-network being studied.

The simulations and results presented in the following paragraph have been made through an extremely powerful software that we implemented in the Matlab environment.

VI. Simulations and Results

With a view to inquire about the consequences of a randomness disturbance on the dynamic behavior of the studied system (IEEE 14 Buses Network), we placed the five machines in a nominal operating condition, at full load, and this from the moment $t_{pr} = 80$ s when a permanent regime is established in these machines. The power base of the studied system is $S_B = 100MVA$. In steady state, the voltage module and phase at different buses is shown in table I, $MS_1 = 615MVA$ is considered as a reference machine.

TABLE I. Voltage module and phase at different buses

Bus	$V_i, i=\{2,...,14\}$	$\alpha_i, i=\{2,...,14\}$
*bus*2	0.9489	-0.0927
*bus*3	0.8630	-0.2554
*bus*4	0.8785	-0.2004
*bus*5	0.8927	-0.1684
*bus*6	0.8200	-0.3160
*bus*7	0.8299	-0.2841
*bus*8	0.8299	-0.2841
*bus*9	0.8069	-0.3321
*bus*10	0.7995	-0.3379
*bus*11	0.8051	-0.3309
*bus*12	0.8006	-0.3413
*bus*13	0.7947	-0.3434
*bus*14	0.7775	-0.3676

Simulated disturbance is an additional call of the total active power consumed P_{CT}.

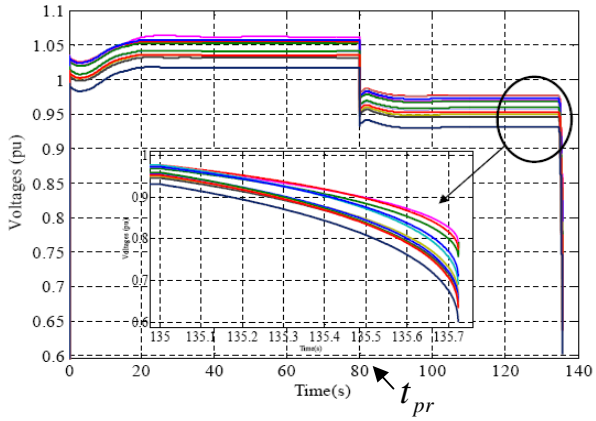

Fig. 14. Voltage levels in case of an additional call of active power

The disturbance simulated consists in engage, at the moment $t_d = 135\ s$, an additional call to active power consumers in all buses. Fig. 14 showed that after seven tenths of seconds, a phenomenon of total voltage collapse appears.

By integration of the new strategy of load shedding, we provided the voltage levels at buses a new steady state and from the moment the fuzzy controllers had judged that the situation tends towards the emergence of the phenomenon of collapse of the voltage from the fact that they have deteriorated sharply, Fig. 15.

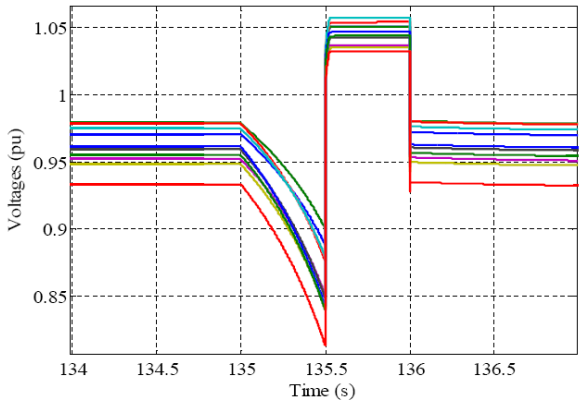

Fig. 15. Temporal evolution of the voltages in the presence of the adopted strategy

Indeed, the term A_{V2k} (11) is instantly adjusted by the new fuzzy load shedding strategy in accordance with the following mathematical model:

$$A_{V2k} = 2.Y_{kk}.\left\{\begin{array}{c}[P_{SM_k} - (1 - \sum_{j=1}^{j=N_m} U_{Cj} \to k).P_{C_k}].\cos(\theta_{kk}) \\ + Q_{IN_k}.\sin(\theta_{kk})\end{array}\right.$$

Which leads to an optimised adjustment of the characteristic path (P_{INk}, V_k), thus avoiding the phenomenon of voltage collapse. Moreover, the frequency of service of the machines have evolved into tolerable margins [$49.9 \le f \le 50.1$] and that during the interval of occurrence of the fault materialized by the additional call of active power, Fig. 16.

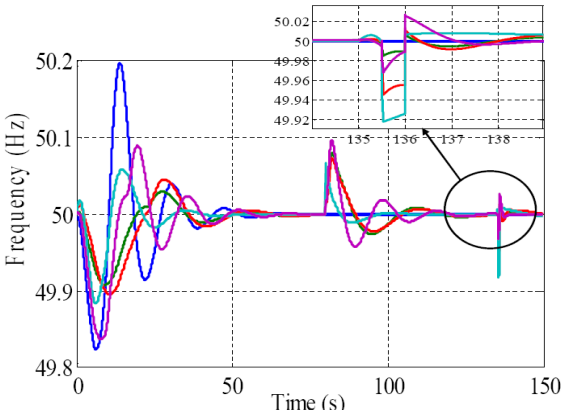

Fig. 16. Temporal evolution of the frequencies of five machines in the presence of the fuzzy load shedding strategy

The frequency stability shown in Fig. 16 is justified by the position control of the intake valves of the turbines, (32). The highest and lowest amplitudes $A_{f_k}^{\max}$ and $A_{f_k}^{\min}$ recorded during frequency fluctuations are determined by the terms:

$$\left\{\begin{array}{l} A_{f_k}^{\max} = \dfrac{\Delta P_{(SM/M)_k}^{\max}}{2.\pi.D_k} + f \\ A_{f_k}^{\min} = \dfrac{\Delta P_{(SM/M)_k}^{\min}}{2.\pi.D_k} + f \end{array}\right.$$

Taking into account the fuzzy load shedding actions incurred, these amplitudes are as follow:

$$\begin{cases} A_{f_k}^{\max} = \dfrac{P_{IN_k} + \left[1 - \sum_{j=1}^{j=N_m} U_{Cj} \rightarrow k\right]^{\max} .P_{C_k} - P_{M_k}}{2.\pi.D_k} + f \\ A_{f_k}^{\min} = \dfrac{P_{IN_k} + \left[1 - \sum_{j=1}^{j=N_m} U_{Cj} \rightarrow k\right]^{\min} .P_{C_k} - P_{M_k}}{2.\pi.D_k} + f \end{cases}$$

In addition, we have allocated a special significance to another type of defect, serious, evidenced by the opening of the line 1-5. This line provides a high level of power flow by liaising the most powerful machine ($MS_1 : 615\,\text{MVA}$) to the rest of network. This defect has been engaged at time $92\,s$ and persisted until the instant $92.01\,s$, Fig.17.

This defect leads implicitly to the phenomenon of voltage and frequency collapse. Implementing this new fuzzy load shedding strategy led to steady state voltages at buses of the network studied Fig. 17.

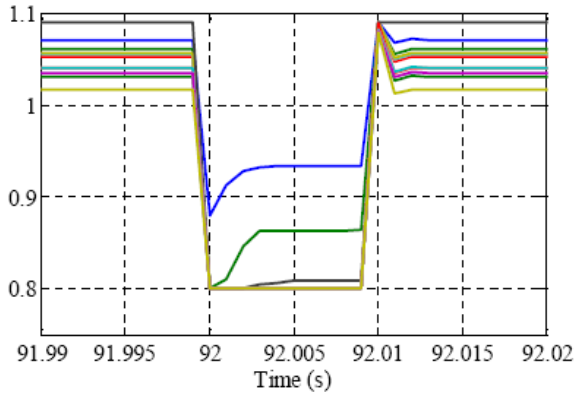

Fig. 17. Voltage levels following the opening of the line 1-5

As for the frequency behavior of different machines, it proves that they maintain a perfect synchronization with the network during the time of opening of the line (1-5) that the magnitudes attained by their frequency $A_{f_k}^{\max}$ and $A_{f_k}^{\min}$ remain bounded by extrema tolerable, Fig. 18.

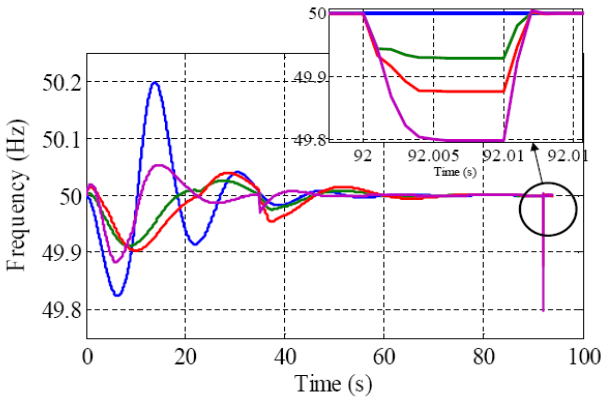

Figure 18. Frequencies of five machines in case of opening of the line 1-5

The temporal evolution of the real parts of eigen values of state matrix $[A_k]$, for the machine MS_2, just further justify the potential performance of the fuzzy load shedding strategy in the case of increased charges, Fig. 19.

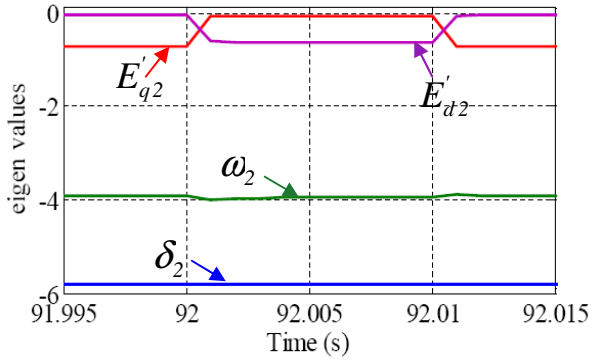

Figure 19. Temporal evolution of the real parts of eigen values of the machine-2 (60 MVA)

VII. CONCLUSION

In this work we developed a new fuzzy load shedding strategy based on perfect estimate margins of variations of state variables of a studied power system, IEEE test network, as it is affected by a disturbance of varying severity. We have attached particular importance to the dynamic behavior of each machine when it is assigned by a random disturbance. Indeed, an adequate mathematical development has allowed us to express the extended margins of power exchanged by each of these machines according to the voltage levels at any network bus. Our main concern was the identification of optimal operating point that could cause the phenomenon of voltage collapse see the blackout. To achieve this, we made recourse to

fuzzy controllers dealing in a first phase margins powers mentioned and their changes over time and a decision would be made by such fuzzy controllers on the amount of charges to be shedded in order to ensure an optimum equilibrium of the production-consumption balance. The basic idea of mathematical development with which we relied in order to create such a strategy has been focused on two major entities namely minimizing the number of fuzzy controllers' involved on one hand and the allocation of increased performance actions of these regulators on the state variables to control on the other. We reported on the impressive potential of such a strategy of shedding that even in case of occurrence of serious defects, opening line, call for additional powers, etc.., The machines are virtually insensitive to the impact of these defects and therefore, we were able to avoid the network studied the phenomenon of voltage collapse. The objectives of this work were achieved and prospects, in the same context, remain promising.

REFERENCES

[1] R. Faranda, "load shedding: New Proposal" IEEE Transactions On Power Systems, VOL.22.NO.4, NOVEMBER 2007.

[2] D. K. SUBRAMANIAN,"Optimum load shedding through Programming techniques ", IEEE Transactions On Power Apparatus And Systems, Vol. PAS-90, NO. 1, JAN-UARY/FEBRUARY 1971.

[3] T.Tomasic, G.Verbic and F. Gubina"revision of the underfrequency load-shedding sheme of the Slovinian power system" IEEE ,2005.

[4] C.J.Parker, I.F.Morrison and D.Sutanto,"Simulation of load shedding as a corrective action against votage colapse",Electrical Power System Research, Elsevier 22. pp 235-241,1998.

[5] M. ISMAIL, M. Mustafa HASSAN "Load Frequency Control Adaptation Using Artificial Intelligent Techniques for One and Two Different Areas Power System" International Journal of Control, Automation and Systems IJCAS, Vol. 1, NO. 1, january 2012, p12-p23.

[6] A. M.A.Haidar,A. Mohamed and A. Hussain,"Vulnerability control of large scale interconnected power system using neuro-fuzzy load shedding approach",Expert Systems With Applicatons, Elsevier 37.pp. 3171-3176, 2010.

[7] A. A.Girgis, S. Marthure,"application of active power sensitivity to frequency and voltage variations on load shedding",Electric Power Systems Reseearch, Elsevier 80 .pp. 306-310,2010.

[8] A.N.Udupa,G.K.Purushothama,K.Parthasarathy and D.Thukaram,"A fuzzy control for network overload alleviation", Electrical Power and Energy System,Elsevier l23.pp. 119-128,2001.

[9] S. –J.Huang, C.-C.Huang,"An adaptative load shedding method with time-based design forisolated power systems", Electrical Power and Energy Systems,Elsevier 22. Pp. 51-58,2000.

[10] P. Kundur "power system stability and control", Electric power research institute,Power System Engineering Series,ISBN 0-07-035958-X, McGraw-Hill,Inc.

[11] P.M. Anderson and A.A.Foued, "Power System Stability and Control",IEEE Press Power Systems Engeneering series ,The institute of Electrical and Electronics Engineers,Inc., New York.445 Hoes Lane,PO Box 1331 Piscataway, NJ 08855-1331.

[12] L.N. Hannett and B. Fardanesh," Field Tests To Validate Hydro Turbine-Governor Model Structure And Parameters",IEEE Transactions on Power System, Vol. 9. No. 4, November 1994.

[13] O. Castillo, P. Melin, J. Kacprzyk and W. Pedrycz," Type 2 Fuzzy Logic : Theory and Applications", IEEE International Conference on Granular Computing, 2007.

[14] A. M.A. Haidar, A. Mohamed, and A. Hussain, "Vulnerability control of large scale interconnected power system using neuro-fuzzy load shedding approach," Expert Systems with Applications, vol. 37,no. 4, pp. 3171–3176, 2010.

[15] Oscar Castillo, Patricia Melin, Jausz Kacprzyk, Wiltold Pedrycz," Type 2 Fuzzy Logic : Theory and Applications", IEEE International Conference on Granular Computing, 2007.

[16] Xuan Wei, Joe H. Chow, B. Fardanesh and Abdel-Aty Edris,"A Dispatch Strategy for a Unified Power-Flow Controller to Maximize Voltage-Stability-Limited Power Transfer", IEEE Transactions On Power Delivery, VOL. 20, NO. 3, JULY 2005.

[17] H. Jouini, S. Chebbi, and K. Jemaï,"Voltage Stabilisation of Electrical Network by Using UPFC Compensator Commanded by Fuzzy Controllers", International Review of Electrical Engineering (I.R.E.E), Vol. 6, N. 2, March-April 2011.